Available online at www.sciencedirect.com
SCIENCE DIRECT®
Journal of Power Sources 138 (2004) 327–339
JOURNAL OF POWER SOURCES
www.elsevier.com/locate/jpowsour

A selective equalizer for NiMH batteries

A. Hande [a,*], T.A. Stuart [b]

[a] Lake Superior State University, USA
[b] University of Toledo, USA

Received 28 April 2004; accepted 25 May 2004
Available online 4 August 2004

Abstract

A unique method has been developed to equalize nickel metal hydride (NiMH) battery packs using a new selective equalizer. This equalizer detects batteries either at a very low state of charge (SOC) or at an extremely high SOC. In this system a set of electromechanical relays is connected in a matrix to route boost current to the weaker batteries. The relay switching is controlled by a 32 bit microcontroller, and the boost current is supplied by a boost charger. Once a weak battery is detected, it is scheduled for a specific boost time by a special "Round Robin" (RR) algorithm. The equalizer was tested on a pack of 12 series connected 12 V 93 ampere hour (Ah) NiMH batteries. Test results show that the equalizer was able to re-balance an artificially unbalanced pack, and the capacity was increased by 27% within six charge–discharge cycles. Results indicate the number of cycles required to re-balance the pack was significantly reduced by using this technique.

Keywords: NiMH; Batteries; Equalizer

1. Introduction

Electric and hybrid electric vehicles (EVs and HEVs) use electrochemical secondary batteries which are connected in series packs to store energy for propulsion. The cell design, ambient temperature, and length of usage/storage are a few factors that affect the life or charge retention of these batteries [1]. This means that if there are certain subtle differences between the individual batteries, the batteries will not charge/discharge in a uniform manner. The result is that some units will be overcharged, some excessively discharged, and poor performance will result.

All batteries obviously must remain within a high and low voltage operating range to prevent damage. During the discharge cycle, batteries which are less efficient tend to go out of voltage balance before the rest, resulting in an overall limiting of the total battery capacity. Similarly, during the charge cycle, batteries which are more efficient tend to get charged a little higher than the rest, resulting in an overcharge. Batteries that are overcharged are subject to an oxygen recombination cycle at their negative electrodes, and this causes their cycle life to be significantly reduced over a period of time [1]. Since the entire battery pack is exposed to a number of charge and discharge cycles, the after effect of these differences results in faster aging of the batteries due to overcharge and undercharge.

These charging and discharging imbalances pose an enormous problem for HEVs. Trickle charging is probably the most common method used to correct these imbalances. The battery pack is first given a bulk charge at a high current and then a trickle charge at a low current [2] of 1 or 2 A. However, this is time consuming since the duration of the trickle charge is usually a few hours. Another scheme is to implement a battery management system (BMS) which monitors certain parameters, such as the voltages and temperatures of individual batteries, and then takes corrective action whenever an imbalance arises. For many types of batteries, the BMS simply monitors the voltage of each battery in the pack, and selects the lowest voltage battery for equalization. This technique is sometimes called selective equalization, and it works very well for batteries such as lead acid and lithium ion where there is a linear relationship between voltage and SOC.

However, one of the more popular batteries used in today's HEVs is the NiMH, and these batteries do not have a linear voltage–SOC relationship. In fact, their voltage is almost constant over most of their SOC range. Therefore, it is very difficult to identify weaker batteries using the conventional

* Corresponding author. Tel.: +1-906-635-2598; fax: +1-906-635-6663.
E-mail address: ahande@lssu.edu (A. Hande).

0378-7753/$ – see front matter © 2004 Elsevier B.V. All rights reserved.
doi:10.1016/j.jpowsour.2004.05.058

selective equalization technique. However, selective equalization can still be used for equalizing NiMH by using a fairly simple algorithm that detects weaker batteries at the end of the charge and discharge cycles, and schedules them for a boost charge in a "Round Robin" (RR) manner.

2. Battery equalization

Several equalization methods are available, including the resistor shunt equalizer [3], re-circulating equalizer [4], electronic (boost) equalizer [5–7], ramp equalizer [8,9], and selective buck-boost equalizer [10]. In all of these equalizers, the main criterion for equalization is the battery voltage, i.e., the cell with the highest or lowest voltage is picked for equalization. All of these techniques are quite effective for batteries such as lead acid or lithium ion where there is a linear relationship between voltage and SOC.

As noted earlier, the voltage versus SOC characteristic for NiMH batteries is very different from lead acid or lithium ion. Fig. 1 shows a typical voltage versus depth of discharge curve for a 12 V 100 ampere hours (Ah) Saft NiMH battery [11] where the voltage is fairly constant for most of the discharge cycle (this is called the voltage plateau). Because of this relatively flat voltage plateau, in practice it is impractical to detect a weak battery on the basis of its voltage except at very low or high SOC values. In a large series connected battery pack there actually could be several batteries with slightly lower voltages but higher SOC values than others with slightly higher voltages. This effect is aggravated by the fact that batteries with a slightly higher impedance show a higher voltage during charging, and a lower voltage during discharging.

The limitations of previous equalizers indicate that a new type of equalizer is required for NiMH batteries. As noted earlier, this new equalizer detects weak batteries either at very low or extremely high SOC values and schedules them for a boost. Weak NiMH batteries can easily be detected at these SOC values because they tend to go out of voltage balance with respect to the other modules in the pack. This new equalizer uses a special algorithm that routes boost current to the weaker batteries in a "Round Robin" fashion rather than giving each battery a complete boost. Thus, every weak battery gets some boost without excessive delays. This technique means that during the subsequent discharge cycles, more ampere hours can be taken out of the weaker batteries. Further cycling might result in the pack being limited by different batteries.

In this system, electromechanical relays and a separate boost charger were used to route the boost current to the weak batteries. A 32 bit Motorola M68376 microcontroller was used to implement the above tasks although a small 8 bit micro probably would have been adequate. The microcontroller controls relay switching in addition to performing various other functions, such as sensing the voltages and temperature of each battery, transmitting data to a personal computer for display, and controlling the charging and discharging process based on the manufacturer's specifications.

3. The selective boost equalizer

The block diagram of the selective boost equalizer is shown in Fig. 2. The equalizer was tested on 12 12 V series connected Saft NiMH batteries (B_1-B_{12}) rated at 93 Ah with a typical voltage range of 6–17 V (V_{min} = 6 V and V_{max} = 17 V). The 32 bit microcontroller first detected the weak batteries, i.e., batteries that bring the discharge cycles to a premature end. When a weak battery was detected, a digital signal was sent from the microcontroller I/O port to a control logic interface circuit. This signal represents a number that indicates the battery selected to receive the next boost. The control logic interface circuit decodes the signal and turns on the required relays in a relay matrix module to route the boost current from a charger to the selected battery. A personal computer was used to display and store relevant data

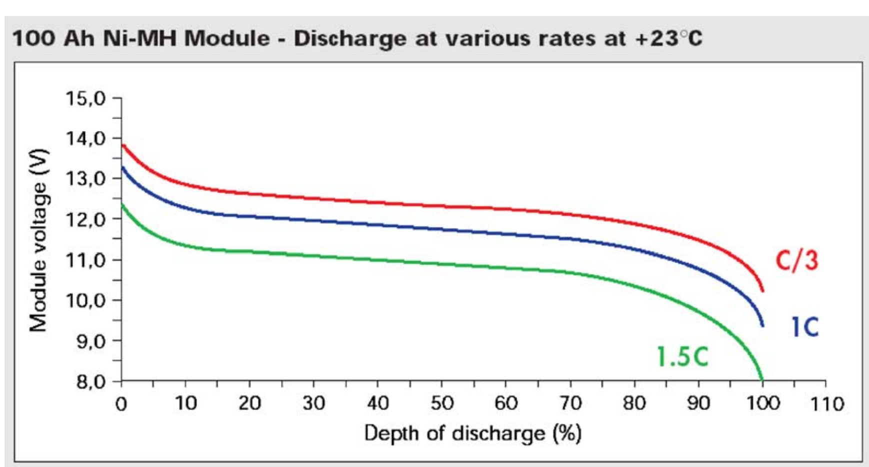

Fig. 1. Typical discharge curve for NiMH batteries.

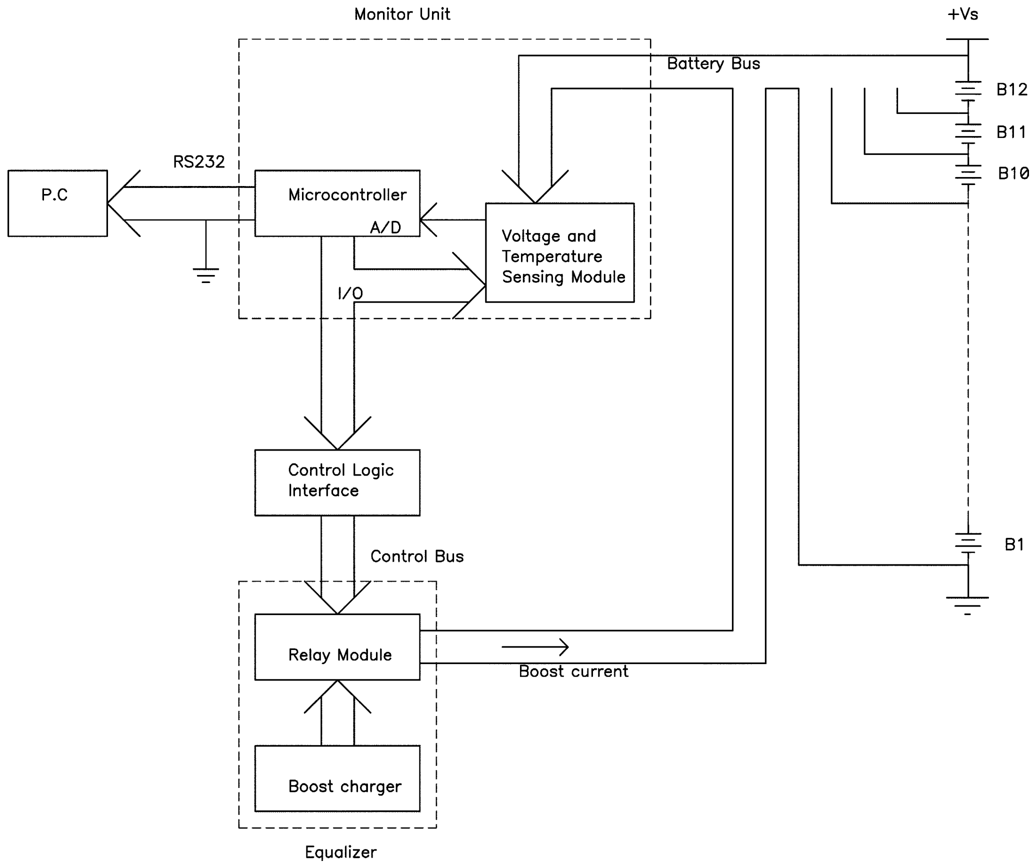

Fig. 2. Selective boost equalizer system.

such as the voltage and temperature of each battery module, charge/discharge current, pack SOC, and so on. Small sealed telecommunication relays were used to achieve high reliability and low cost.

The 12 battery voltages have to be scaled before inputting them to the microcontroller analog-to-digital converter (ADC) since the maximum ADC voltage is only 5 VDC. A voltage divider circuit with 14 and 36 kΩ resistors (shown in Fig. 3) was used for this purpose to produce a scaling factor of 0.28. Therefore, the voltage from a voltage divider will always be less than 0.28×17 V, i.e., 4.76 V. These V_{B_1}–$V_{B_{12}}$ outputs were fed to the inputs of 12 isolation amplifiers (U_1–U_{12}) shown in Fig. 4. Isolation amplifiers were used because all of the scaled voltages except V_{B_1} are above ground and have to be shifted to the same reference level as the ADC. Fig. 5 shows the ADC circuit with a 16 channel multiplexer (AD7506) to route the isolated voltage signals V_1–V_{12} to the microcontroller ADC via the PQB0 line. Port A (PQA7–PQA0) of the microcontroller was configured as an 8 bit digital output port, and PQA3–PQA0 were used as the address bus for selecting the appropriate voltage lines (V_1-V_{12}) for measurement.

Fig. 6 shows the relay matrix module comprised of seven relays, and Fig. 7 shows the control logic interface module consisting of a set of FETs (Q_1-Q_7), two latches and eight NAND gates. The relays in the matrix module are shown in the OFF (normally closed) position. PQA0–PQA5 (Port A of microcontroller) were used to output a 6 bit binary number that represents the weak battery that needs a boost. Table 1 shows the binary numbers for each of the 12 batteries. This number indicates the relays to be turned ON in order to route the boost current to the selected weak battery. The 6 bit binary number is latched at the outputs of the two CD4042 latches during a negative clock transition at their CLK inputs. PQA7 and PQA6 (Port A of microcontroller) are used for the data latching operation. This latching

Table 1
Logic table for battery selection

Battery	PQA0	PQA1	PQA2	PQA3	PQA4	PQA5
B_{12}	0	0	0	0	0	1
B_{11}	0	0	0	1	0	1
B_{10}	0	0	0	1	1	1
B_9	1	0	0	0	0	1
B_8	1	0	0	1	0	1
B_7	1	0	0	1	1	1
B_6	0	0	1	0	0	1
B_5	0	0	1	1	0	1
B_4	0	0	1	1	1	1
B_3	0	1	1	0	0	1
B_2	0	1	1	1	0	1
B_1	0	1	1	1	1	1

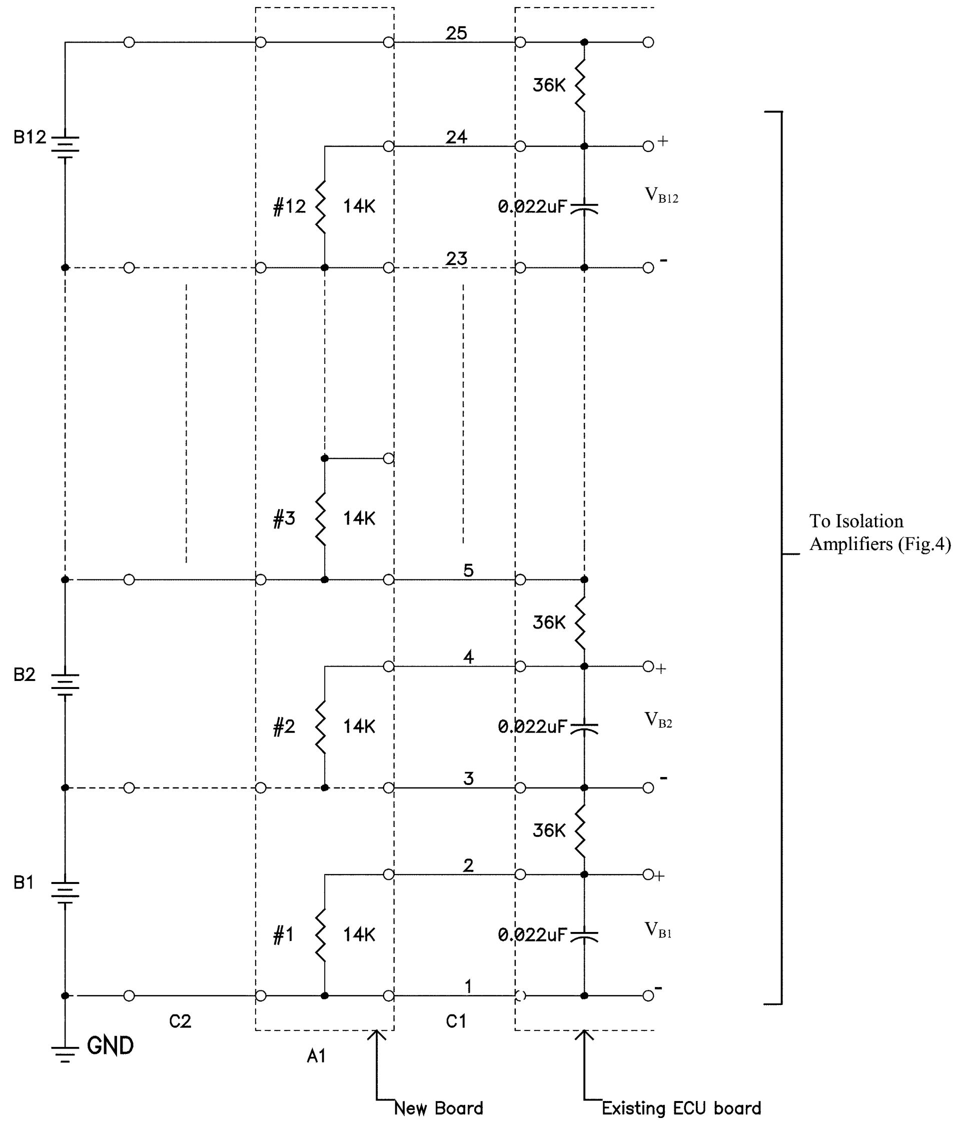

Fig. 3. Voltage scaling circuit.

operation causes the corresponding FETs in the control logic interface module to turn ON at the same time, thus energizing their corresponding relay coils. For example, if battery B_5 is detected as the weak battery, the 6-bit data output from PQA0–PQA5 of the microcontroller corresponds to 001101_2 (in binary). This data is then latched onto the outputs of the two CD4042 latches causing FETs Q_3, Q_4, Q_6, and Q_7 to turn ON. Therefore, relays 3, 4, 6 and 7 turn ON, and boost current is routed to B_5. Table 2 shows the relays that turn ON when any of the 12 batteries is detected for a boost. Relays 1, 2, 3, 4, and 7 were driven by signals directly from PQA0–PQA5, respectively. However, relays 5 and 6 were controlled by a set of NAND gates in conjunction with microcontroller signals PQA3 and PQA4. This was done in order to perform the function of reversing the polarity for batteries B_2, B_5, B_8, and B_{11}, so that the positive terminals of these batteries are connected to the positive terminal of the boost charger whenever any one of these is selected for a boost.

4. The “Round Robin” algorithm

A special “Round Robin” algorithm was used to control the relays for routing the boost current from the charger to the weak batteries. The program flowchart is shown in Fig. 8. Several key parameters of the equalizer are initialized to appropriate values before commencing the equalization process. The equalizer is initially turned OFF, and the boost time for all batteries is set to zero. After initializing the equalizer parameters, the algorithm sits in an infinite loop and looks for the weakest battery in the pack. Weak NiMH batteries can be identified only at the end of their charge and discharge cycles. This is because over most of

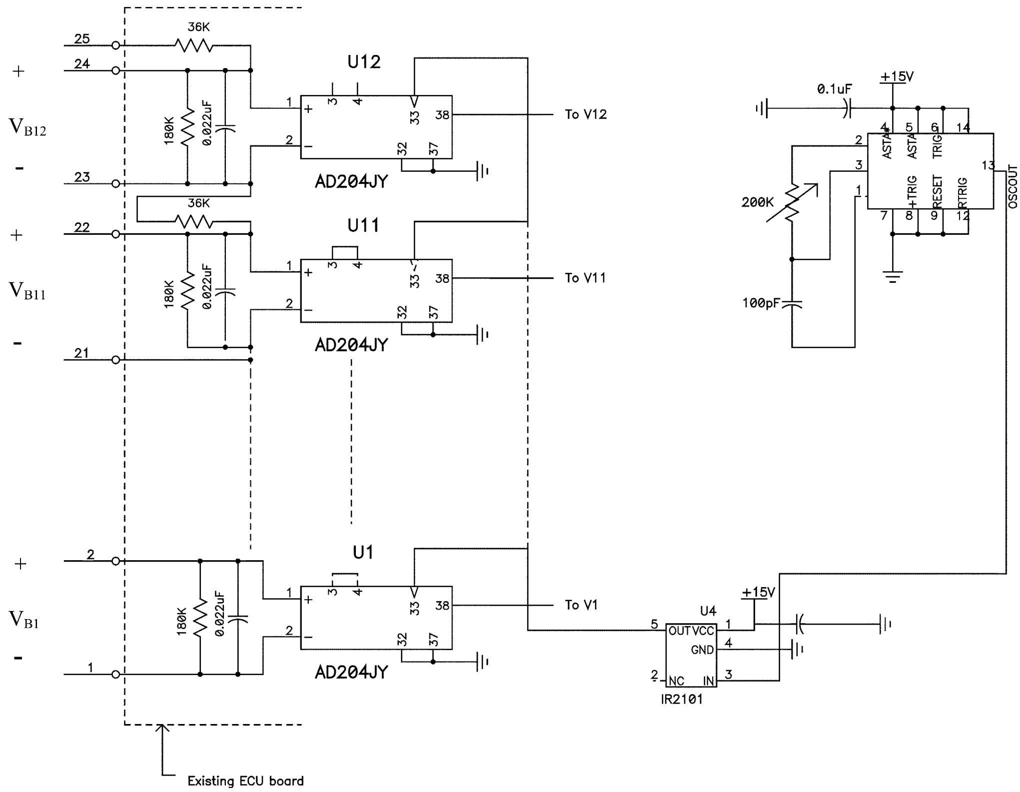

Fig. 4. Isolation amplifier layout.

the SOC range the voltages of all battery modules are fairly constant. Towards the end of charge and discharge cycles the weaker batteries tend to start falling out of voltage balance with respect to the other modules in the pack. During the subsequent cycling tests it was observed that the accelerated increase in the voltages of efficient batteries during the end of the charge cycles did not limit the capacity of the pack. It was the rapid voltage drop of weaker batteries during the end of the discharge cycles that limited the capacity. Tests also showed that the threshold value for detecting these weaker batteries during the discharge cycles was about 0.4 V, i.e, the weaker batteries could be identified when their voltages fell 0.4 V below the average pack voltage. Therefore, the "Round Robin" algorithm detects a weak battery when ($V_{avg} - V_{min}$) > 0.4 V, where V_{avg} is the average voltage of batteries, and V_{min} is the voltage of weakest battery.

After detecting the weak battery, it is scheduled for a boost of '*x*' amperes for a total boost time of '*y*' minutes. The algorithm then switches the corresponding relays in the relay matrix to route boost current to the detected weak battery, and starts a new boost session. While the weak battery is being boosted, the equalizer continues to search for other weak batteries. If other such batteries are detected during this time, their boost times are also set for '*y*' minutes. However, they must wait for the current boost session to end before they receive any boost current.

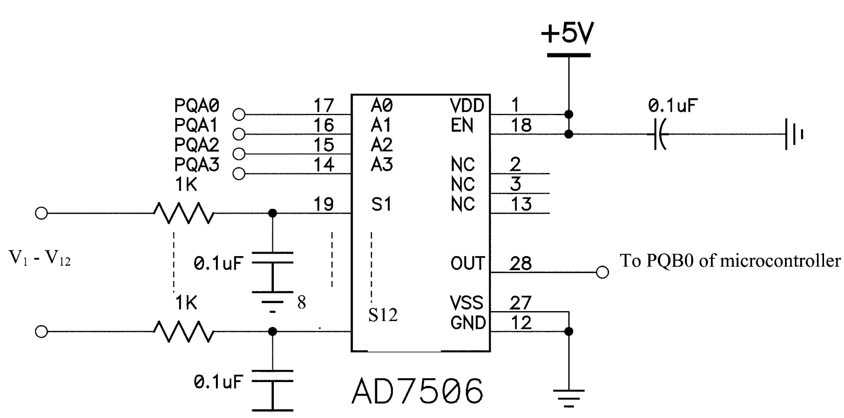

Fig. 5. Analog-to-digital conversion (ADC) circuit.

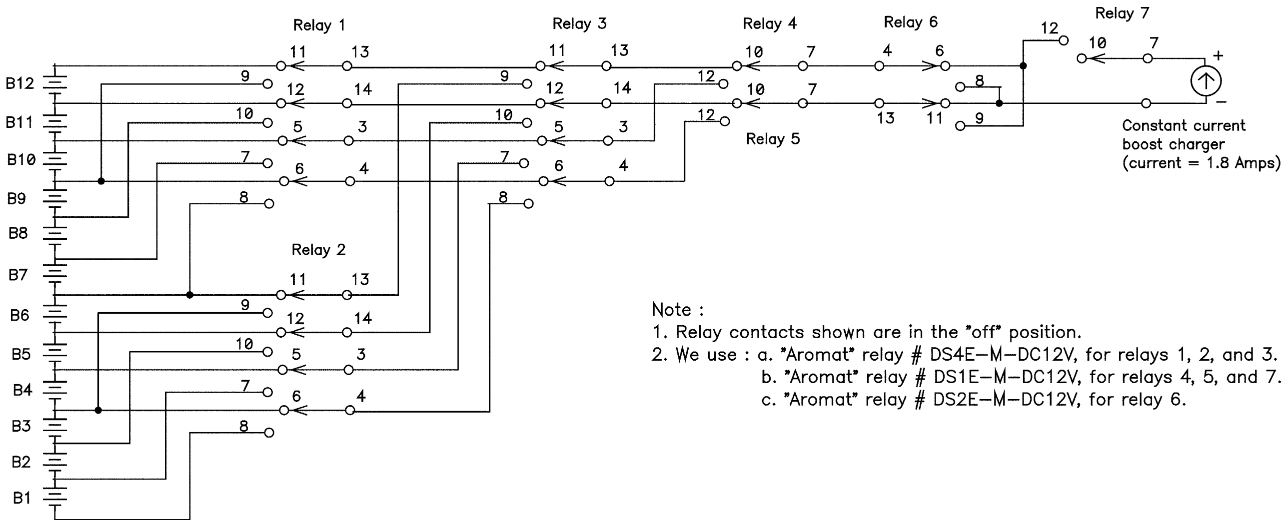

Fig. 6. Relay matrix module.

While current is being supplied to the battery currently under boost, the present boost session is updated. Fig. 9 shows the flowchart depicting all the processes that get updated during a boost session. The boost time for the battery currently under boost is decremented, and the time elapsed for the present boost session (on time) is incremented. After 'z' minutes ($z < y$), the algorithm turns the equalizer OFF by turning all the relays in the relay matrix to their OFF

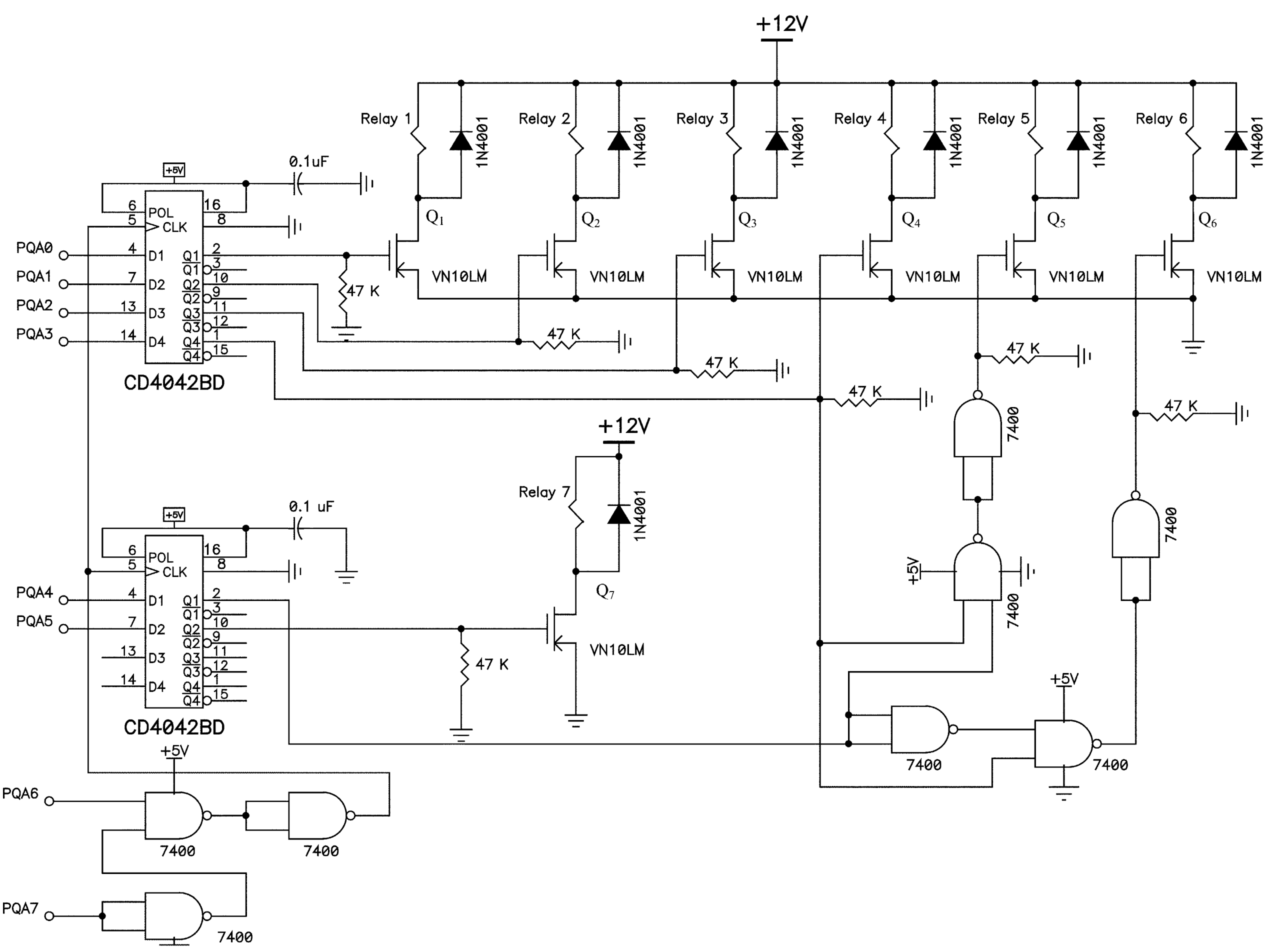

Fig. 7. Control logic interface module.

Table 2
Logic table for relay selection

Battery	Relay 1	Relay 2	Relay 3	Relay 4	Relay 5	Relay 6	Relay 7
B_{12}	0	0	0	0	0	0	1
B_{11}	0	0	0	1	0	1	1
B_{10}	0	0	0	1	1	0	1
B_9	1	0	0	0	0	0	1
B_8	1	0	0	1	0	1	1
B_7	1	0	0	1	1	0	1
B_6	0	0	1	0	0	0	1
B_5	0	0	1	1	0	1	1
B_4	0	0	1	1	1	0	1
B_3	0	1	1	0	0	0	1
B_2	0	1	1	1	0	1	1
B_1	0	1	1	1	1	0	1

1 = relay ON; 0 = relay OFF.

positions. It then increments the battery number and checks whether the next battery has any boost time left. For example if battery B_1 was being boosted for 'z' minutes, the algorithm stops boosting B_1 and checks whether B_2 has any boost time left. It keeps incrementing the battery number until it finds a battery with some boost time remaining. If a new weak battery is found, the algorithm turns ON the required relays in the relay matrix and starts boosting this new weak battery. If multiple weak batteries are detected, each battery is boosted only for 'z' minutes instead of its complete quota of 'y' minutes. Therefore, each weak battery does not have to wait too long for its turn for a boost, and the pack is balanced in a more efficient manner. This process continues until each weak battery has no boost time remaining, i.e., each weak battery has received a complete boost = xy Ah.

The RR algorithm, therefore, sits in an infinite loop boosting the detected weak batteries until the boost times for all the batteries are zero. This algorithm also can be used to boost any type of battery by varying the values for boost time, on time, and boost current. Since the boost current is routed through the relays, its value is limited by their maximum current carrying capability. These experiments used 12 V 1.8 A telecom type Aromat relays in the relay matrix. Therefore, the boost current was limited to 1.8 A, but other relays would allow higher current ratings. The values for "boost" time and "on" time should not be too long or the newly detected weak batteries may have to wait for an excessive amount of time before receiving a boost. If the boost is too short it may lead to excessive relay switching, which may decrease the lifetime of the relays.

5. Experimental system and procedures

A block diagram of the system is shown in Fig. 10. Separate wires were used for voltage sensing, temperature sensing, and boost equalizing. The voltage sensing lines and boost charging lines were connected to the batteries via 2 A fuses. Chilled water was circulated through the batteries during pack cycling using a 4.3 gal/min chiller. The chiller was used to maintain the battery temperatures within the specified limits during cycling. A dc power supply was used for charging the pack and a variable resistive load was used for discharging. Charge cycles were carried out using a bulk charge of 29 A and a trickle charge of 4.7 A. The power supply output current and its ON/OFF operation were controlled by the microcontroller based on voltage and current measurements. The load was controlled manually during discharge to produce a discharge current of approximately 50 A for most of the discharge cycle. Towards the end, the load resistance was gradually increased until the discharge current decreased to about 15 A. This procedure was used in order to extract a slightly higher charge from the pack during discharge. The duration and amount of current allowed to flow through the pack during the charging and discharging cycles were based on the battery manufacturer's specifications.

The power supply current was controlled by an analog voltage during the charge cycles. A voltage, V_2, of 0–100 mV applied to the control terminals corresponded to an output current (I_o) of 0–50 A (Fig. 11). V_2 was controlled by the microcontroller using a digital-to-analog converter (DAC0830) to produce the following relationship:

$$V_2 = \frac{-V_1 100\,\Omega}{5\,\mathrm{k}\Omega} - \frac{V_1}{50} \quad (1)$$

$$\text{where} \quad \pm V_1 = \pm V_{REF} \times \pm\text{digital code from microcontroller} \quad (2)$$

The ON/OFF control circuit for the dc power supply is shown in Fig. 12.

6. Experimental results

The technique of boosting the weak batteries individually for a specified period during charging and discharging was first tested using a relatively simple method. During these initial tests, if more than one weak battery was detected, the

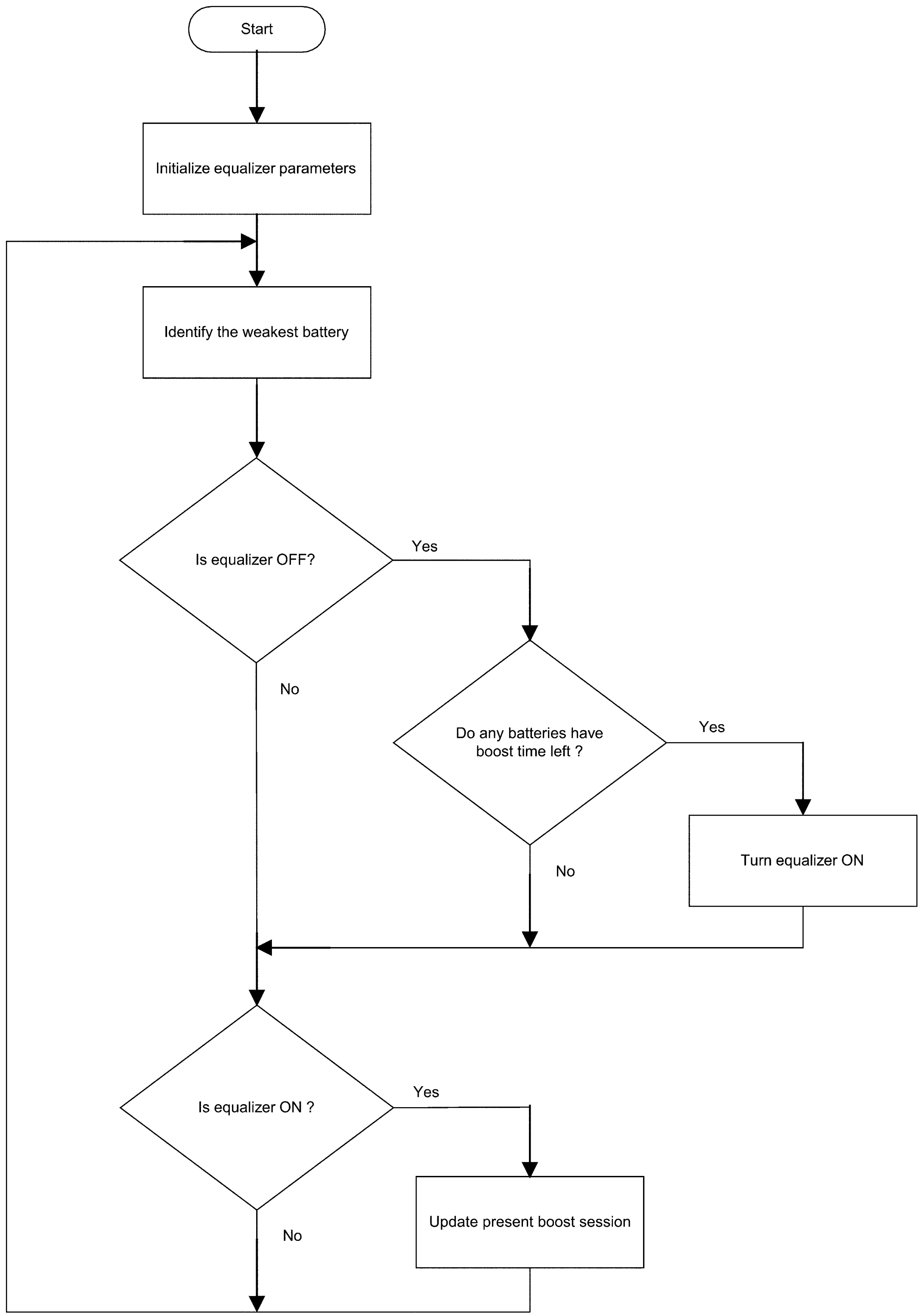

Fig. 8. “Round Robin” algorithm flowchart.

first battery was given a complete boost before attending to any of the others.

The 12 V NiMH batteries used in these tests had a capacity rating of 93 Ah. About 10% of the rated Ah, i.e., approximately 9 Ah was removed from one of the batteries (B_7) after the pack had been fully charged. This was done to create an artificial unbalance in the pack so that the equalizing process could be effectively tested. The pack was then

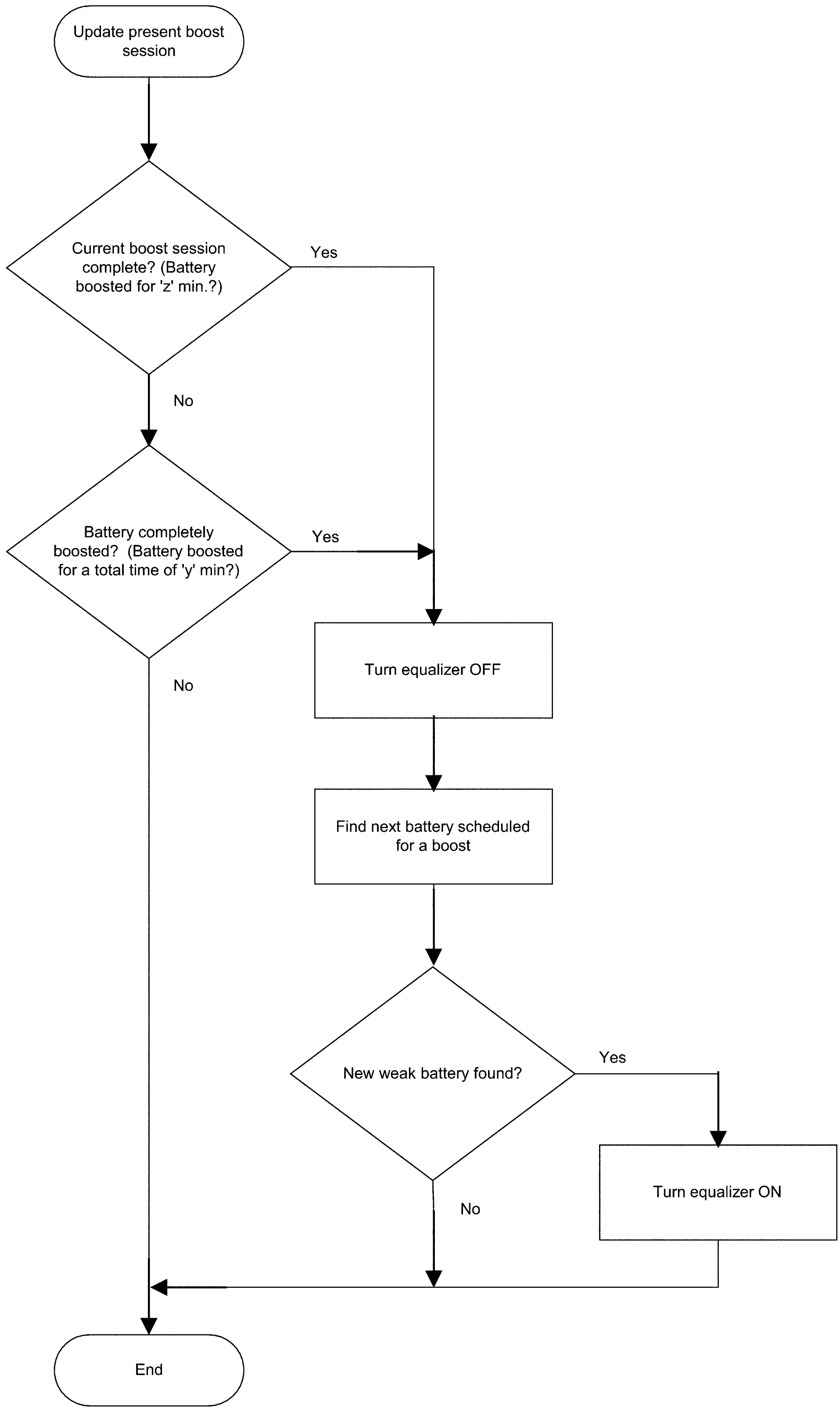

Fig. 9. Update present boost session flowchart.

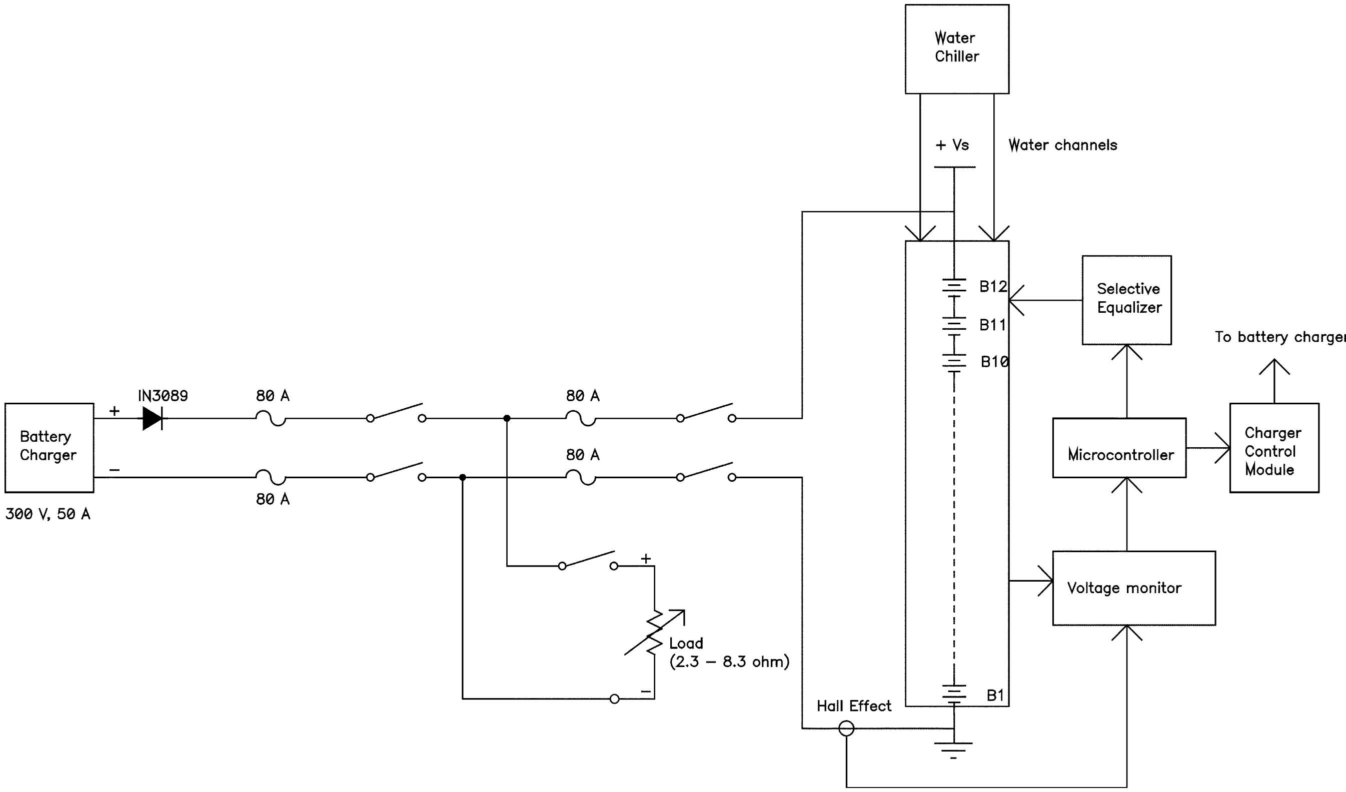

Fig. 10. Experimental system.

cycled, and as expected, at the end of discharge cycle #1, B_7 was observed to be the first to show an abrupt voltage drop. A boost current of 1.8 A was then applied to B_7 for about 5 h to insure that the total Ah added to the weak battery was about 9 Ah. Actually, in practice the proper Ah of boost would be very difficult to determine for this simple algorithm. This is because the optimum Ah boost should be only slightly greater than the Ah of the unbalance which, of course, is unknown. If the boost is much greater than the unbalance, significant energy loss will occur due to overcharging, and if it is too small, balance will not be achieved. The previously described RR algorithm could reduce this problem because the boost is applied in several smaller "doses". Overcharging would thus be reduced if the doses were discontinued once the battery was no longer detected as a weak unit.

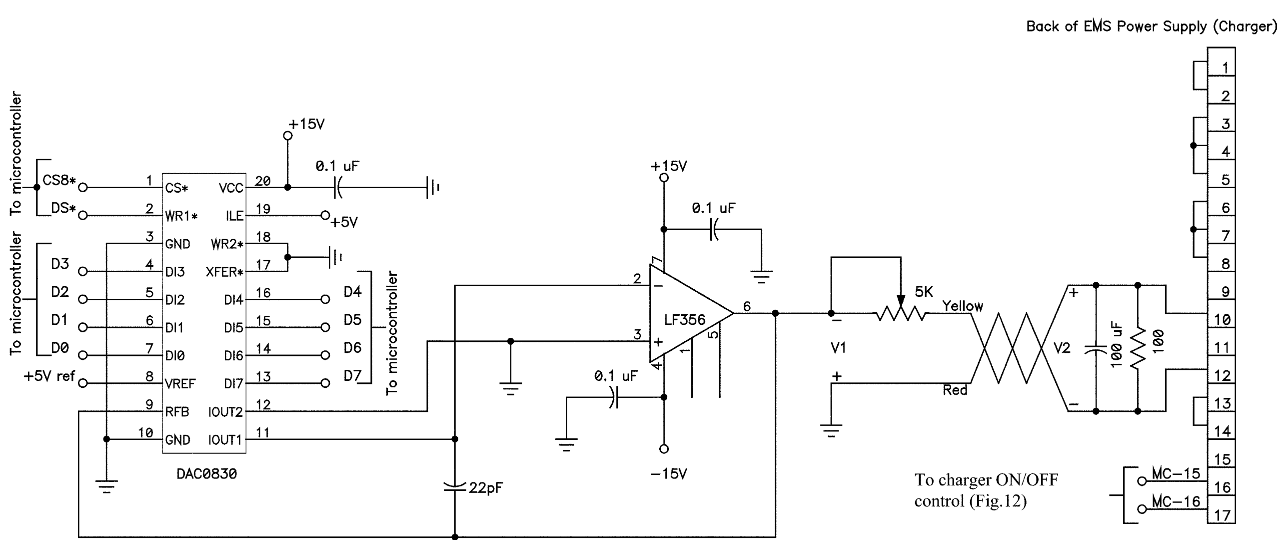

Fig. 11. Power supply current control circuit.

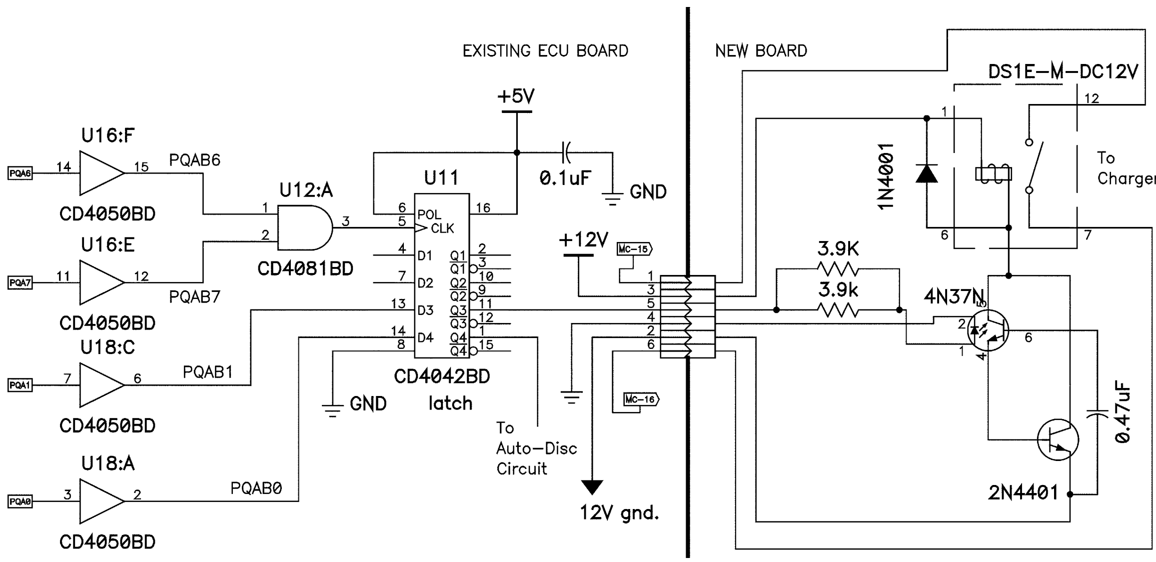

Fig. 12. Power supply ON/OFF control circuit.

The discharge Ah of the pack was then recorded at the end of each cycle. During cycle #2, battery B_7 received a complete boost, and therefore it was not detected as the weakest battery. In fact B_8 was detected and scheduled for a boost. The discharge Ah improved to 86.4 Ah. During the subsequent discharge cycle, i.e., #3, the Ah improved to 88.31, but B_7 was detected again. In fact, it was observed that as the SOC of the pack approached close to 100%, either B_7 or B_8 was detected as the weak battery. This may have occurred because B_7 and B_8 had a slightly higher impedance than the other batteries, causing their voltages to be slightly lower during the discharge cycles. The discharge Ah of the pack increased from 81 to 92.8 Ah (SOC $\cong$ 100%) after six charge and discharge cycles as shown in Fig. 13.

Obviously, several different techniques can be used for boosting the batteries. During the above tests using the first equalization method, a complete boost of 9 Ah was given to battery "*x*" before proceeding to battery "*y*". This worked fairly well when only one or two batteries were scheduled for a boost (Fig. 13), but further tests revealed that if three or more batteries are scheduled, the procedure is less effective. This is because the boost is not uniformly distributed among the defective batteries. This results in some of the batteries getting a complete boost before the commencement of the next discharge cycle, while the rest might not yet receive any boost. This was observed during the tests that used the first equalization method where only one battery was purposely unbalanced. This unbalanced battery, as expected, was detected at the end of discharge cycle #1 and received a complete boost during the subsequent discharge cycle. Although the pack capacity improved, other batteries (especially those with slightly higher impedances) were detected and scheduled for a boost. When one or two such batteries were scheduled for a boost, the discharge capacity of the pack increased gradually until it equaled about 93 Ah (Fig. 13). As mentioned before, in most of the tests either B_7 or B_8 were found to be the weak batteries as the SOC approached 100%. The Ah obtained during the subsequent

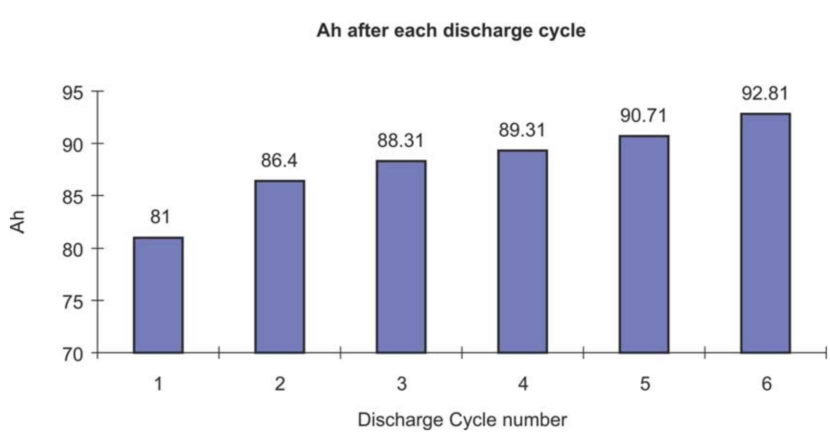

Fig. 13. Equalization results without "Round Robin" algorithm.

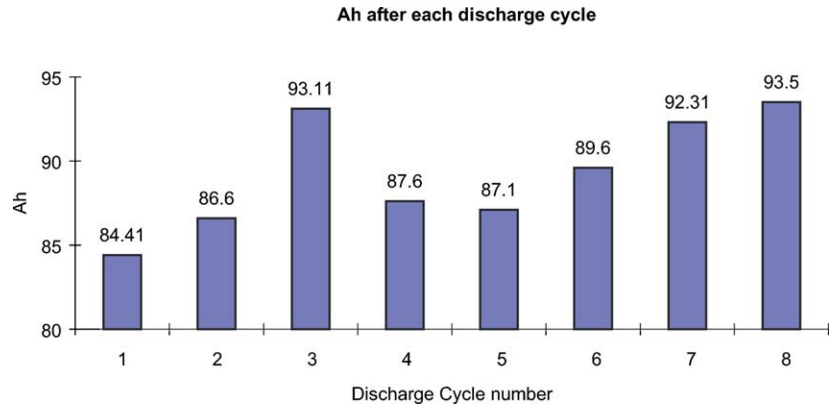

Fig. 14. Equalization results without “Round Robin” algorithm.

discharge cycles remained close to 93 Ah. However, in one test where B_3 was purposely unbalanced, slightly different results were obtained. In this test, three weak batteries were detected when the SOC equaled 100%. This caused the Ah in the following discharge cycle to be much lower.

Fig. 14 shows the results obtained where 9 Ah was purposely taken out from one battery (B_3) to create an artificial unbalance in the pack. As expected, battery B_3 was detected for a boost at the end of discharge cycle #1. During cycle #2, battery B_3 got a complete boost. Therefore, at the end of discharge cycle #2, B_3 was not detected to be the weakest battery. In fact two other batteries, B_7 and B_8, were detected and were scheduled for a boost, and the Ah recorded at the end of discharge cycle #2 improved to 86.6. During the subsequent discharge cycle, i.e., #3, the Ah improved to 93.1 (SOC $\cong$ 100 %), but the microcontroller detected three weak batteries viz. B_7, B_9, and B_{10}. Battery B_7 was scheduled for a boost again because it did not receive a sufficient amount of boost during the previous cycle (discharge cycle #3). Although the pack SOC was approximately equal to 100%, it was decided to observe the effect of these three weak batteries on the discharge Ah by continuing the pack cycling. The algorithm first started boosting B_7 during cycle #4. However, it failed to completely boost battery B_9 and B_{10} before the commencement of cycle #5. As a result, battery B_9 was detected for a boost again at the end of discharge cycle #4, and the capacity of the pack decreased to 87.6 Ah. With further cycling the capacity improved gradually from 87.6 to 93.5 Ah (SOC $\cong$ 100%) because in each of the subsequent cycles viz. #5–8, either battery B_7 or B_8 was detected for a boost, and it was boosted completely before the start of the following cycle.

To counter the above problem, it was decided to boost the defective batteries using the RR algorithm. Three batteries (B_5, B_9 and B_{10}) were purposely unbalanced (9 Ah was taken from each of them) in order to test the algorithm. During discharge cycle #1, the algorithm detected the above three batteries and scheduled them for a boost. The boost current was then routed through the relays in accordance with the RR algorithm guidelines described earlier. The boost current was set to 1.8 A and the boost time for each detected battery was set to 5 h so that the total Ah added to each battery equaled 9 Ah. The RR algorithm boosted the detected batteries in small “doses” of 54 m each, until the boost times for all batteries equaled zero. The period of each dose was selected to be 54 m so that about 1.6 Ah (18% of

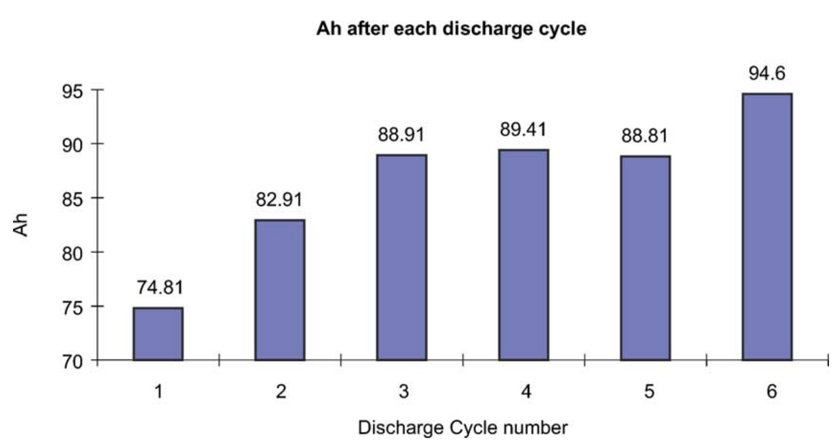

Fig. 15. Equalization results with “Round Robin” algorithm.

the total 9 Ah unbalance) was added during every dose. The capacity increased from 74.8 to 94.6 Ah (slightly above the 100% SOC rating) after six charge and discharge cycles [12] as shown in Fig. 15.

The total number of cycles required for the artificially unbalanced pack to be re-balanced were thus significantly reduced using the RR algorithm. This occurred even though the RR algorithm test had three purposely unbalanced batteries, whereas the previous test only had one. Additional testing might indicate better values for the RR algorithm's boost time, "dose" time, and current, and this remains a topic for further study.

7. Conclusions

The new selective equalizer proved to be very effective for equalizing the 12 series connected NiMH batteries. The technique used for equalization is a universal one and is not restricted to one particular type of battery. This is because the equalization principle does not follow the traditional method of picking the cell with lowest voltage for equalization, but instead looks for batteries that initiate the end of the charge and discharge cycles. Several tests were carried out in order to evaluate this equalizer. The traditional technique of boosting a weak battery completely before attending to another weak battery worked reasonably well, but the time required to equalize the pack was reduced even further by using the RR algorithm. The optimum amount of boost current and time will differ from battery to battery, and this depends on a variety of factors such as the individual battery characteristics and SOC ratings.

The equalizer is compact and makes use of inexpensive components. Moreover, it can be broken down into modularized units located close to the batteries so that each unit serves a particular section of the battery pack. Since HEVs require several series connected batteries, these modularized versions [13,14] are probably the best choice for future implementation. The lifetime of relays used was rated at a minimum of 5×10^5 switching operations at a current of 2 A [15]. Based on the much lower number of expected switching operations, this indicates the equalizer should easily outlast the life of an HEV. The voltage sensing module in these tests used twelve isolation amplifiers for measuring individual battery voltages. The cost and size of the voltage sensing unit can be drastically reduced by using cheaper techniques such as a voltage transfer circuit [16,17] or an op amp transfer circuit [18] instead of these isolation amplifiers. The need for separate boost lines could be eliminated by locating the equalizer closer to the pack and also using the voltage sensing lines for boosting the batteries.

Acknowledgements

This research was supported jointly by grants from the US Department of Energy National Renewable Energy Laboratory (grant no. ACI-9-29118-01) and DaimlerChrysler, AG. The authors also would like to acknowledge the advice and assistance provided by Dr. Cyrus Ashtiani and Mr. Giovanni Bolgiani from DaimlerChrysler.

References

[1] D. Linden, Handbook of Batteries and Fuel Cells, McGraw-Hill, 1995.
[2] M. Fukino, N. Irie, H. Ito, Development of an Electric Concept Vehicle with a Super Quick Charging System, SAE Paper No. 920442, 1992.
[3] M.H. Moody, A high reliability battery management system, J. Power Sources 18 (1986) 223–231.
[4] S.T. Hung, D.C. Hopkins, C.R. Mosling, Extension of Battery Life via Charge Equalization Control, IEEE Trans. Ind. Electron. 40 (1) (1993) 96–104.
[5] R. Park, Method of Equalizing the Voltages of Individual Cells of Storage Batteries, US Patent 4331991 (25 May 1982).
[6] N.H. Kutkut, D.M. Diwan, D.W. Novotny, Charge equalization for series connected battery strings, IEEE Trans. 31 (3) (May/June) (1995) 562–568.
[7] N.H. Kutkut, D.M. Diwan, H. Wiegman, D.W. Novotny, Design considerations for charge equalization of an electric vehicle battery system, IEEE 1995, APEC Proceedings, March 1995, pp. 96–103.
[8] Z. Ye, An electronic equalizer for series connected batteries, Ph.D. Dissertation, The University of Toledo, December 1995.
[9] T. Gottwald, Z. Ye, T. Stuart, An High Frequency Electronic Equalizer for EV and HEV Batteries, Future Transportation Technology Conference, Paper Number 972636, San Diego, CA, August 1997.
[10] M. Tang, T. Stuart, Selective buck-boost equalizer for series battery packs, IEEE Trans Aerospace Electron. Sys. 36 (1) (January) (2000) 201–211.
[11] Nickel-Metal Hydride Modules for Electric Vehicles, Saft Inc., http://www.saftbatteries.com/130-Catalogue/PDF/HE_NIMH.pdf.
[12] A. Hande, A selective boost equalizer for NiMH batteries, Masters Thesis, The University of Toledo, May 2000.
[13] X. Wang, A modular battery management system, Ph.D. Dissertation, The University of Toledo, May 2001.
[14] T.A. Stuart, C. Ashtiani, A. Pesaran, F. Fang, X. Wang, A Modular Battery Management System for HEVs, SAE Future Car Congress, Paper Number 2002-01-1918, Arlington, VA, June 2002.
[15] Highly Sensitive 1500 V FCC Surge Withstanding Miniature Relays, Aromat Corporation, http://www.aromat.com/pcsd/ds.pdf.
[16] D.B. Garrett, A localized voltage monitoring scheme for a series battery pack, Masters Thesis, The University of Toledo, December 1998.
[17] D.B. Garrett, T.A. Stuart, Transfer circuit for measuring individual battery voltages in series packs, IEEE Trans. Aerospace Electron. Sys. 36 (3) (July) (2000) 933–940.
[18] X. Wang, T.A. Stuart, An Op amp transfer circuit to measure voltages in battery strings, J. Power Sources, 109 (2) (July) (2002) 253–261.